2022

Measurement of Orientation and Distance Change Using Circularly Polarized UWB Signals

Janusz Przewocki
University of Gdansk, janusz.przewocki@ug.edu.pl

Max Ammann
Technological University Dublin, max.ammann@tudublin.ie

Adam Narbudowicz
Trinity College Dublin, Ireland, narbudoa@tcd.ie

Recommended Citation

J. Przewocki, M. J. Ammann and A. Narbudowicz, "Measurement of Orientation and Distance Change Using Circularly Polarized UWB Signals," in IEEE Transactions on Antennas and Propagation, vol. 70, no. 6, pp. 4803-4809, June 2022, doi: 10.1109/TAP.2022.3140500.

Funder: Science Foundation Ireland

Measurement of Orientation and Distance Change Using Circularly Polarized UWB Signals

Janusz Przewocki, Max J. Ammann, *Fellow, IEEE*, and Adam Narbudowicz, *Member, IEEE*

***Abstract*— The article proposes methodology to use circularly polarized (CP) ultra-wideband (UWB) signals for simultaneous measurement of orientation and distance changes between transmitter and receiver. The proposed technique uses the rotational Doppler effect on CP pulsed communication. The amplitude of a CP signal is immune to polarization misalignment in the presence of rotation; however, the phase is subjected to a frequency-invariant shift proportional to the rotation angle. This significantly distorts the pulse shape in the time domain and can be used for the measurement of the rotated angle. By combining the technique with the well-known localization capability of UWB systems, one can precisely measure not only the distance but also the orientation. This is demonstrated by both numerical and experimental studies presented in this article.**

***Index Terms*— Circular polarization, localization, remote sensing, ultra-wideband (UWB).**

I. Introduction

CIRCULARLY POLARIZED (CP) signals are routinely used where the orientation of transmit and receive antennas is unknown or changes with time [1], since the amplitude of the CP signal is invariant to signal rotation. However, so far there are limited studies on the implications of the rotation on the phase of CP signals. First, in [2] it was demonstrated for optical signals that a CP signal rotation will produce a phase shift – a phenomenon known as angular Doppler effect or rotational Doppler effect [3].

For radio signals, it was observed in [4] that the effect can be used to monitor orientation and rotation of objects within a very large range of rotational speeds. In the experimental setup, the target was fixed at a constant distance, as any distance change would have caused a phase delay and consequently an error in measurement, i.e., the system in [4] is unable to distinguish between the phase shift due to rotation and distance change.

In contrast to the classical Doppler effect, its angular counterpart produces a phase shift that is constant and frequency-invariant, i.e., rotation by angle α between the transmitter and receiver results in the same phase shift of α at all frequencies that are CP. This principle was used in a dual-frequency numerical study in [5]; however, the measurement results were prone to a significant error due to lack of redundancy. In [6], a qualitative discussion noted that a CP ultra-wideband (UWB) pulse will be distorted in the presence of rotation. While it provides no quantitative results, it suggests the possibility of simultaneous measurement of the orientation and distance using such pulses. This capability would allow robust measurements over a significantly greater distance than currently available coupling sensors [7]–[9].

Furthermore, due to the popular use of UWB signals for very precise localization [10]–[13], the localization and orientation measurement could be combined into a single system that provides full information about the tagged object. With the rapid development of low-cost UWB CP antenna technology, e.g., [14]–[16], such systems could be beneficial for multiple applications.

This article investigates for the first time the practical use of UWB CP signals [17] for simultaneous measurement of the orientation and distance change between the transmit and measured antennas. It significantly extends the results from [6] by demonstrating that by analyzing the UWB CP pulse phase, one can accurately determine both the orientation and distance changes in the presence of noise. The presented theory validates the performance of the technique for various axial ratios (AR), bandwidths, and signal-to-noise ratios (SNRs). The experimental verification in a semi-anechoic environment shows a mean angle error of $-2.7°$ with a standard deviation of $1.76°$ and a mean distance error of -0.3 mm with a standard deviation of 0.3 mm. The system is intended to expand the readily available capability of UWB localization with orientation sensing. This is intended mainly for an integrated radio-navigation system for robotic and drone systems that are expected to form the core of Industry 4.0 manufacturing. The tag that is placed on the moving and rotating object needs to incorporate only a wideband transmitter with a CP Tx antenna, with all computation executed at the receiver (Rx) side. The weight of the Tx antenna is only 16 g. The system is expected to operate up to 50 m distance without exceeding the power levels allowed by FCC UWB standard (assuming

Manuscript received March 15, 2021; revised November 9, 2021; accepted December 20, 2021. Date of publication January 5, 2022; date of current version June 13, 2022. This work was supported by the Science Foundation Ireland under Grant 18/SIRG/5612. *(Corresponding author: Adam Narbudowicz.)*

Janusz Przewocki is with the Faculty of Mathematics, Physics and Informatics, University of Gdansk, 80-308 Gdansk, Poland (e-mail: janusz.przewocki@ug.edu.pl).

Max J. Ammann is with the Antenna and High Frequency Research Centre, School of Electrical and Electronic Engineering, Technological University Dublin, Grangegorman, Dublin D07 ADY7, Ireland.

Adam Narbudowicz is with the CONNECT Research Centre, Trinity College Dublin, Dublin 2, D02 PN40 Ireland, and also with the Department of Telecommunications and Teleinformatics, Wroclaw University of Science and Technology, 50-370 Wroclaw, Poland (e-mail: narbudoa@tcd.ie).

Color versions of one or more figures in this article are available at https://doi.org/10.1109/TAP.2022.3140500.

Digital Object Identifier 10.1109/TAP.2022.3140500

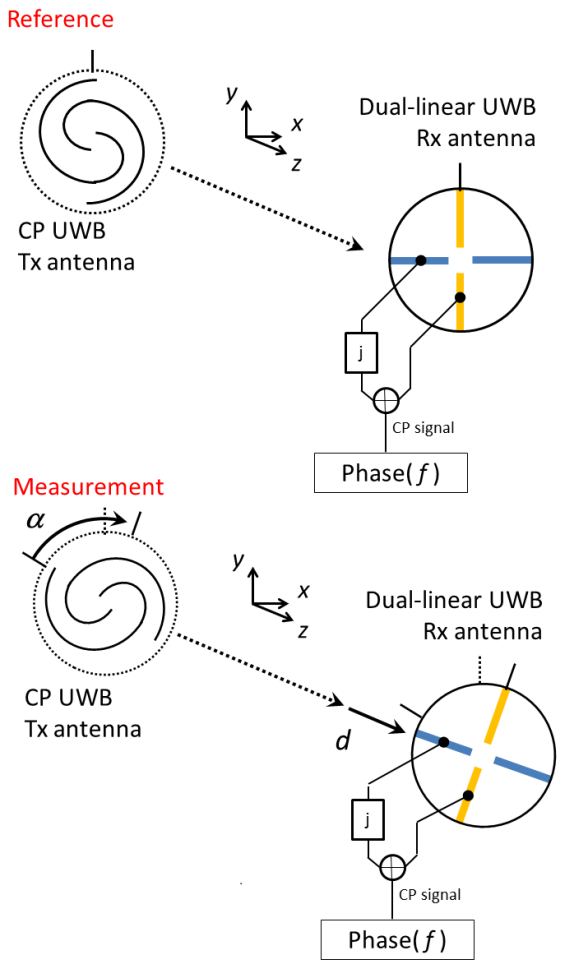

Fig. 1. Scheme of the investigated scenario, with the dual-polarized UWB receive antenna changing its orientation α and distance along z-axis Δz.

receive antenna with 12 dBic gain, i.e., similar to the one used in this study).

II. Mathematical Model

A. Time-Domain Analysis of UWB CP Signals

Fig. 1 depicts the investigated scenario with two measurements: the reference measurement M1 to record the initial position/orientation and measurement M2 executed after applying a relative displacement and/or rotation to the antenna. The proposed technique compares the phase shift at different frequencies of the pulse, which eliminates the need for high fidelity of the radiated UWB pulse.

The transmit antenna is an UWB CP antenna, i.e., it radiates a CP signal within the FCC UWB spectrum mask from 3.1 to 10.6 GHz. Assuming an idealized case where antenna's transfer function is negligible, the transmitted CP pulse can be depicted as a superposition of two orthogonal linearly polarized pulses: E_x and E_y [17]. The two orthogonal components have the same spectral magnitude and are phase shifted by 90° at all investigated frequencies, producing the Axial Ratio (AR) of 0 dB for every frequency involved.

The receiving (Rx) antenna is a dual linearly polarized UWB antenna, measuring two orthogonal linear components (denoted as E_p and E_q). The circular polarization at the receiver (Rx) is recovered by post-processing as in [18, (1)], i.e., the E_p signal forms imaginary part, while the E_q signal forms a real part of the right-handed CP signal. This approach minimizes error due to AR variation in the receiver. For successful calculation, only the phase of the CP signal as a function of frequency f is recorded. The displacement and orientation change is calculated by comparing the phases of the two measurements, with the calculation details outlined in subsequent sections.

B. Rotation and Displacement

The receive antenna (Rx) is displaced along the z-axis by distance d and is rotated along the same axis by angle α. The effect of translation is well-known and is modeled by applying a time delay to the transmitted pulse. In the presence of rotation α, the relationship of the transmitted signal E_x, E_y to the received E_p, E_q can be described by the following rotation matrix: [19, Example 7.6]:

$$\begin{bmatrix} \cos\alpha & -\sin\alpha \\ \sin\alpha & \cos\alpha \end{bmatrix}. \tag{1}$$

This rotation will significantly distort the shape of the UWB pulse in the time domain. Fig. 2 shows exemplary pulses of E_q- and E_p-components in the Rx antenna. It can be seen that the distortion is substantially different from any distortion due to linear movement. As is subsequently demonstrated, the time delay will produce a phase shift that can be clearly distinguished from the phase shift due to rotational Doppler effect, facilitating a simultaneous measurement of d and α.

In the numerical experiments described in Section III, we compare a reference pulse corresponding to the original position and orientation of the Rx antenna with another pulse received at a new position and orientation of Rx antenna. Based on these data, we estimate linear and angular displacements.

III. Numerical Studies

The first step generates n samples for each of the two Gaussian pulses, corresponding to the orthogonal electric field components E_x and E_y of the CP pulse as outlined in Section II. The pulses' bandwidth is from 3.1 to 10.6 GHz, defined with respect to the full width at half maximum (FWHM) of the amplitude of the signal's spectrum. The time window of the pulses is from -0.5 and 0.5 ns. The number of time-domain samples is $n = 1000$, if not stated otherwise.

The signal is then subjected to angular and linear displacements, as outlined in Section II. The white Gaussian noise with mean value zero and standard deviation σ is added. Since signal's power spectrum is not constant in the frequency domain, we decided to calculate SNR in the time domain. The appropriate formula is

$$\text{SNR} = \frac{s^2}{\sigma^2} \tag{2}$$

where s^2 is the signal sample variance calculated in the time window $[-t_c, t_c]$ where $t_c = 0.19$ ns is the cut-off time for

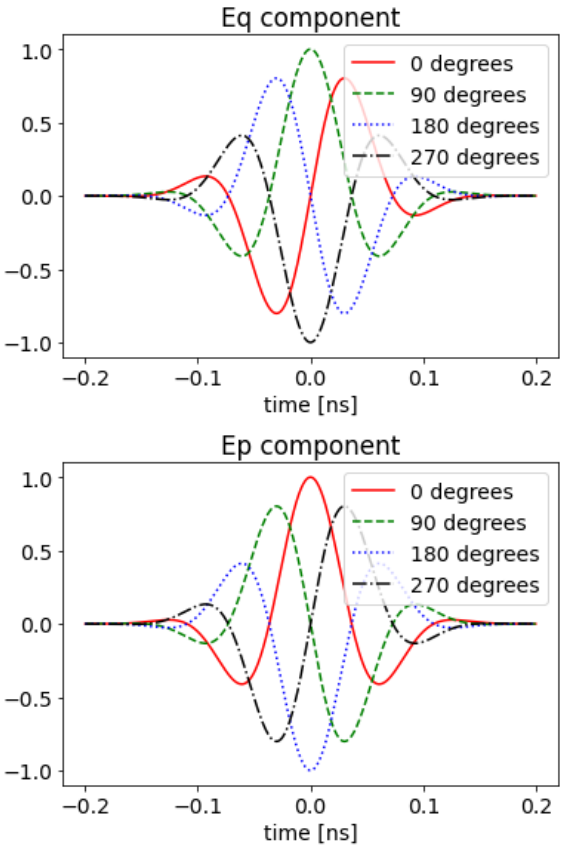

Fig. 2. Pulses received for E_q- and E_p-components' different rotations α.

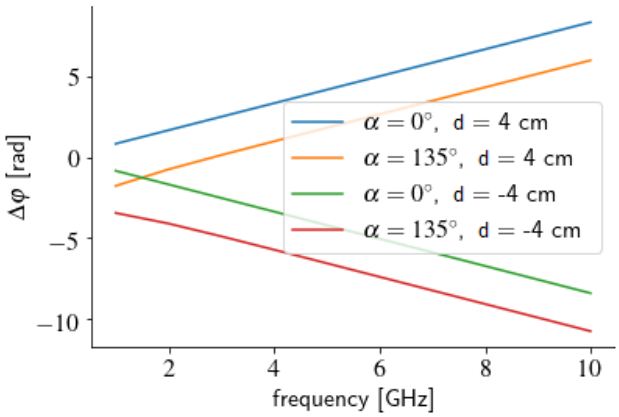

Fig. 3. Phase differences $\Delta\phi(f)$ for exemplary pulses without noise.

signal's strength below -60 dB with respect to the maximum value. Note that in many full-wave simulators threshold of about -40 dB is used. Here, we take lower value for better accuracy.

The signal is then analyzed on the receiver side to compute angular and linear displacements. This information is contained in the phase difference with respect to the reference pulse. Therefore, both the pulses are transformed to the frequency domain and the phase difference between them $\Delta\phi(f)$ is calculated for each frequency.

Fig. 3 shows phase difference $\Delta\phi(f_i)$ for exemplary pulses with various rotations and displacements. As expected, linear displacement results in a linear dependence between $\Delta\phi$ and frequency f, while angular displacement is related to a constant dependence.

In the presence of noise, one should not expect $\Delta\phi$ to be a linear function of the frequency. Therefore, the least-squares method is used to fit a straight line to the set of data points $(f_i, \Delta\phi(f_i))$, where f_i's are the frequency points belonging to the bandwidth of the transmitted Gaussian pulse.

Let c denote the speed of light in vacuum. Since the signal's time delay due to displacement d is equal to d/c, its phase shift is proportional to frequency f and equals

$$\Delta\phi = 2\pi f \frac{d}{c}. \tag{3}$$

From that, we see that the slope a of the regression of $\Delta\phi$ with respect to variable f is equal $2\pi d/c$. Therefore, we can estimate d with the following formula:

$$d = \frac{a}{2\pi} c. \tag{4}$$

On the other hand, the rotation matrix (1) is frequency-invariant. Therefore, when applied to CP signals, the rotation introduces constant phase shift that allows to estimate the angular displacement α by the intercept point (i.e., constant bias) of the regression line.

To validate the proposed technique, three equally spaced values of the linear displacement in the range from 0 up to 15 mm are selected. The angular displacement is varied from 0° up to 45° with step equal to 5°. For each of these settings, both the parameters are estimated using the proposed linear regression method. Table I shows the absolute errors of the estimated parameters averaged over selected values of linear and angular displacements. Additionally, in Figs. 4 and 5, we show descriptive statistics of the calculated absolute errors. The method was evaluated for three different SNR values: 3, 6, and 9 dB which represent high-noise scenarios.

TABLE I
MEAN ABSOLUTE ERROR ESTIMATED WITH THE LINEAR REGRESSION ALGORITHM

SNR	angular displacement error	linear displacement error
3 dB	7°	0.59 mm
6 dB	6°	0.44 mm
9 dB	5°	0.3 mm

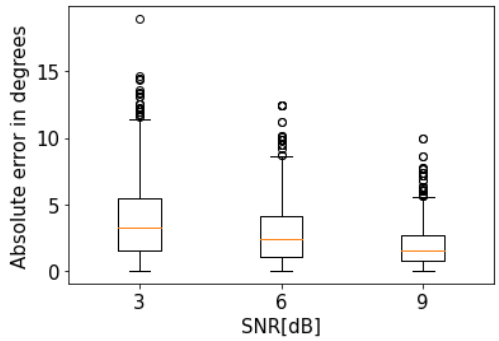

Fig. 4. Absolute error of the measured angular displacement.

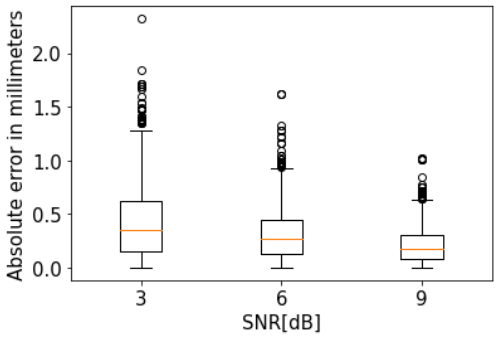

Fig. 5. Absolute error of the measured linear displacement.

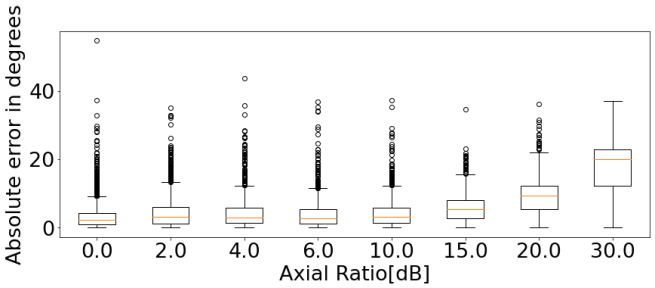

Fig. 6. Absolute error of the estimated angle displacement as a function of AR.

It can be seen that for all the investigated SNR values the system allows good resolution in both angle and distance. For the most noisy case of SNR = 3 dB, the mean angular error is 7° with 75% of samples exhibiting error of 5° or less. For SNR = 9 dB, the respective errors are 5° and below 4° for 75% of samples. This is considered sufficient for most applications.

The mean errors for distance change are below 1 mm. It should be noted here that this accuracy refers only to the distance change with respect to single antenna. The localization accuracy—as reported in [11]—will exhibit significantly larger errors due to the required distance measurement from at least three different antennas ("anchors"). The exact localization accuracy also strongly depends on the processing algorithm itself and is therefore beyond the scope of this article.

To verify the sensitivity of the proposed technique, the effects of AR, bandwidth and frequency offset were studied. Fig. 6 demonstrates the error of rotation measurement as a function of varying AR. The AR was adjusted by modifying the amplitude of the E_x-component of the transmitted signal. The increase in error for values up to AR = 10 dB is very small, demonstrating good robustness even for a class of elliptical polarization, with stable AR within the investigated bandwidth. This is most likely because the AR impacts mainly amplitudes of the rotating signals, but not the phase differences produced by angular displacement. Therefore, sufficiently low AR is required to ensure sufficient link budget for all the angles throughout the rotation. As long as this is satisfied, further improvements of AR have limited impact on increased accuracy.

For the error in distance change shown in Fig. 7, the AR has no impact.

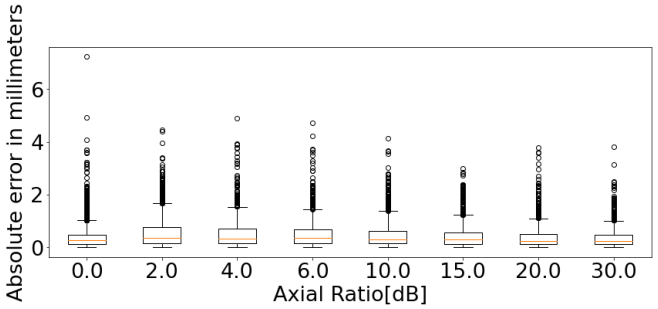

Fig. 7. Absolute error of the estimated shift displacement as a function of AR.

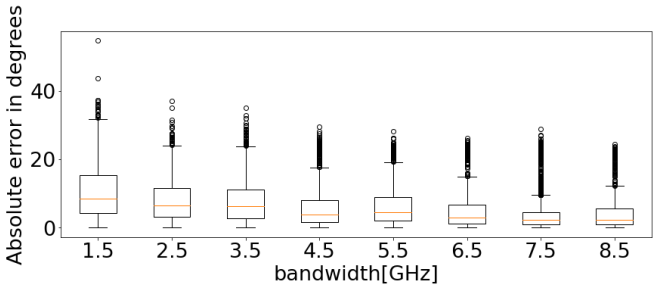

Fig. 8. Absolute error of the estimated angle displacement versus absolute bandwidth.

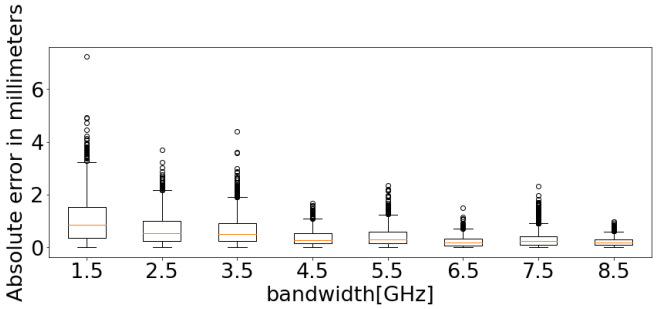

Fig. 9. Absolute error of the estimated linear displacement versus absolute bandwidth.

The bandwidth reduction was simulated by reducing the number of frequency points for linear regression. Figs. 8 and 9 show the effect of bandwidth on the orientation and linear displacement, respectively. As expected from linear displacement theory, the decrease in bandwidth resulted in greater displacement measurement inaccuracy. A similar trend is seen in Fig. 8 for the rotation measurement. For the bandwidth of 2.5 GHz, the errors are 6.5° and 0.48 mm for α and d, respectively.

Finally, the impact of center frequency was investigated by shifting the whole spectrum by up to 200 MHz (i.e., without altering the absolute bandwidth). The study did not reveal any substantial changes in the performance. This is expected, as the phase shift produced by rotation is frequency-invariant [20].

IV. Experimental Results

The experimental setup is shown in Fig. 10. The transmit antenna is compact UWB planar slot antenna [14], with two orthogonal wideband slots fed through an UWB phase shifter. The antenna generates elliptical polarization, with measured

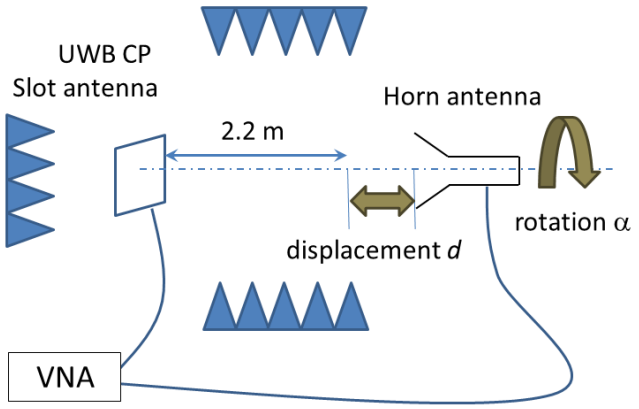

(a)

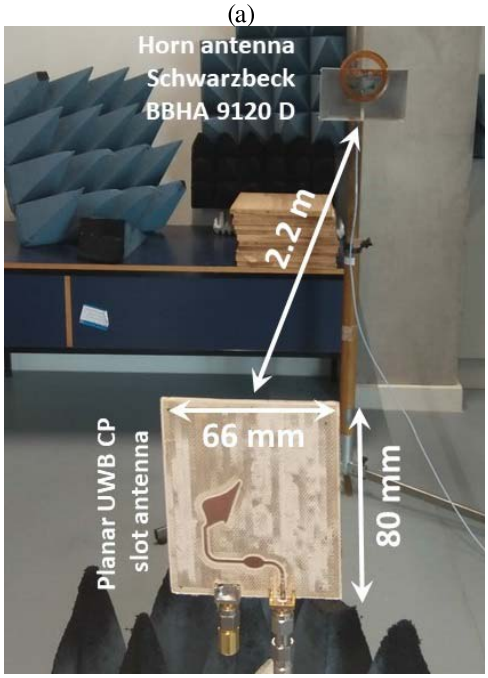

(b)

Fig. 10. Experimental setup of the proposed technique. (a) Schematic view. (b) Picture of the setup with dimensions.

boresight AR in Fig. 12. As can be seen, the AR $<$ 3 dB requirement for circular polarization is not satisfied within the full bandwidth: although two CP minima are visible at 3.5 and 6.6 GHz, there is an increase of up to 8 dB at 5 GHz. Also, for higher frequencies above 9 GHz, there exist ripples in AR up to 25 dB. However, as shown in Fig. 6, the proposed technique can operate within AR $<$ 10 dB with negligible increase in error.

The receive antenna is an UWB ridged horn antenna Schwarzbeck BBHA 9120 D, typically used as a probe for antenna measurements. As it supports single linear polarization, two different measurements are taken for each sample, i.e., for horizontal and vertical polarizations. The experiment is conducted in a concrete-walled open-laboratory space of TU Dublin Grangegorman Campus, with limited number of absorbers located at first-order reflection points. The distance over which the measurement is performed is 2.2 m, with realized gains of both the antennas shown in Fig. 12(b).

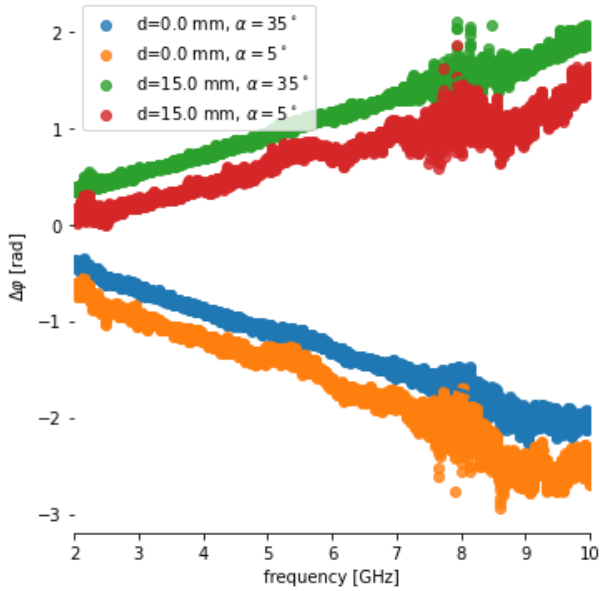

Fig. 11. Measured phase shifts $\Delta\varphi$ for different configurations of Rx antenna and corresponding linear regression lines.

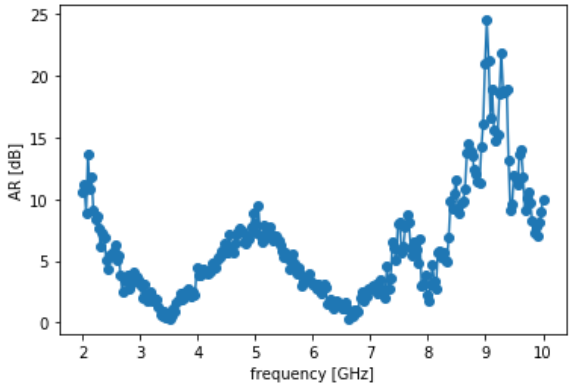

(a)

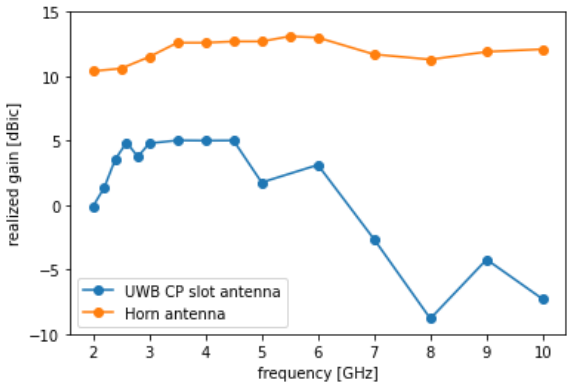

(b)

Fig. 12. Measured antenna parameters. (a) Axial ratio of the transmit antenna. (b) Realized gains of both Tx and Rx antennas.

The gain of the planar UWB CP slot antenna was measured using the three-antenna methodology, while the gain of the horn is given by the manufacturer's data. The size of the UWB CP slot antenna is 66 by 80 cm. Its operating principles and design procedure are described in detail in [14]. It exhibits

TABLE II
ANGLES AND DISPLACEMENTS CALCULATED IN THE EXPERIMENT

d (mm)	α (°)	Estimate of d (mm)	Estimate of α (°)
0.0	0.0	-0.02	359.33
0.0	5.0	0.37	10.67
0.0	10.0	0.43	15.77
0.0	15.0	0.49	20.41
0.0	20.0	0.41	25.09
0.0	25.0	0.38	28.78
0.0	30.0	0.28	33.25
0.0	35.0	0.19	37.39
0.0	40.0	0.05	41.06
0.0	45.0	0.00	45.00
5.0	0.0	5.35	1.89
5.0	5.0	5.65	8.23
5.0	10.0	5.70	13.49
5.0	15.0	5.77	18.53
5.0	20.0	5.75	23.72
5.0	25.0	5.67	28.68
5.0	30.0	5.60	33.27
5.0	35.0	5.63	37.56
5.0	40.0	5.53	42.15
5.0	45.0	5.45	46.70
10.0	0.0	9.67	357.89
10.0	5.0	9.96	5.97
10.0	10.0	10.10	12.39
10.0	15.0	10.19	17.96
10.0	20.0	10.19	23.20
10.0	25.0	10.15	28.18
10.0	35.0	10.00	37.74
10.0	30.0	10.09	33.17
10.0	40.0	9.96	42.26
10.0	45.0	9.83	46.11

relatively low gain, which is a consequence of relatively small structure with wide beamwidth. Although a larger CP antenna with a more selective beam could improve the link budget, for practical application the antenna's size and weight are also a valid concern.

The results are measured as a complex transmission coefficient S_{21} using Rohde & Schwarz ZVA vector network analyzer (VNA). Measured phase shift is shown in Fig. 11. To cover 2–10 GHz bandwidth with 4001 frequency samples, the Rx antenna was subjected to rotation α and displacement d with respect to the initial location and orientation. The experiment combined three values of displacement d varying from 0 to 10 mm with a step of 5 and 10 values of rotation α from 0° to 45° with a step of 5°. This yields a total of 30 combinations shown in Table II.

Contrary to the numerical studies in Section III, the regression was applied in two steps. The rationale behind this was to improve the quality of the method which was impaired by imperfections of real measurements. In the first step, frequency points with amplitude of the received signal below −50 dBm were removed before fitting of the regression line. This was because weak signals produce random phase variation due to division by zero. The goal of the second step was to counteract the influence of outlying points. Here, another regression line was fit after excluding 10% of the data with the largest absolute values of residuals. The accuracy of the proposed method is evaluated by mean error, i.e., an arithmetic average of differences between true values and respective estimates. The precision of the algorithm is evaluated by standard deviation of these differences. The mean angle error is about −2.7° with a standard deviation of 1.76°, whereas the mean distance error is −0.3 mm with a standard deviation of 0.3 mm. The mean errors for angle and distance indicate a slight bias in the measurements, when simultaneously estimating the displacement and rotation angle. However, this bias can be compensated by appropriate calibration. Note that precision is better than the numerical results presented in Table I, which is due to much larger SNR when using VNA. The relative error for distance measurement is 6.7%. This calculation excluded values with $d = 0$ mm, as those would result in division by zero.

TABLE III
COMPARISON OF THE PROPOSED WORK WITH STATE-OF-THE-ART RF ROTATION SENSORS

Work	Rotation meas.	Distance meas.	Range	Reported Angle	precision Distance
[7]	Yes	No	$<$ 1 cm	–	–
[9]	$< 90°$	Yes	$<$ 1 cm	–	–
[21]	$< 180°$	No	0.4 m	$< 5°$	N/A
[4]	Yes	No	0.75 m	1.5°	N/A
[10]	No	Yes	3.5 m	N/A	1 cm
[11]	No	Yes	5 m	N/A	13 cm
			20 m	N/A	23 cm
[13]	No	Yes	8 m	N/A	4.1 cm
This work	Yes	Yes	2.5 m	1.76°	0.3 mm

Table III shows the comparison of the proposed technique with other works that reported various rotation or distance change measurements. In [10], [11], and [13], the precision is reported as the standard deviation, whereas the resolution declared by authors is quoted in [4] and [21]. The "range" column denotes the maximum distance over which the measurement was performed, as reported in respective publications. Overall, most rotation sensors use proximity coupling and are designed to operate over small distances. The UWB displacement measurements offer good accuracy and long range, but so far they we not able to integrate rotation sensing.

V. CONCLUSION

The article proposes a new measurement technique that uses UWB CP signals for simultaneous measurement of distance and rotation. The technique is demonstrated numerically and experimentally using, respectively, 120 and 35 different scenarios with varying distances and orientation angles. The results show very high accuracy of the proposed technique even with distorted AR of the antenna.

REFERENCES

[1] S. Gao, Q. Luo, and F. Zhu, *Circularly Polarized Antennas*. Hoboken, NJ, USA: Wiley, 2014.
[2] B. A. Garetz, "Angular Doppler effect," *J. Opt. Soc. Amer.*, vol. 71, no. 5, p. 609, May 1981.
[3] G. Li, T. Zentgraf, and S. Zhang, "Rotational Doppler effect in nonlinear optics," *Nature Phys.*, vol. 12, pp. 736–740, Oct. 2016.
[4] V. Sipal, A. Z. Narbudowicz, and M. J. Ammann, "Contactless measurement of angular velocity using circularly polarized antennas," *IEEE Sensors J.*, vol. 15, no. 6, pp. 3459–3466, Jun, 2015.
[5] A. Narbudowicz, M. J. Ammann, and D. Heberling, "Simultaneous rotation and distance measurement using multiband circularly polarized radio link," in *Proc. Int. Symp. Antennas Propag.*, 2016, pp. 846–849.
[6] A. Narbudowicz, J. Przewocki, and M. J. Ammann, "On the distortion of UWB circularly polarized time-domain pulses in presence of rotation," in *Proc. IEEE Int. Symp. Antennas Propag. USNC-URSI Radio Sci. Meeting*, Jun. 2019, pp. 1735–1736.

[7] J. Mata-Contreras, C. Herrojo, and F. Martín, "Application of split ring resonator (SRR) loaded transmission lines to the design of angular displacement and velocity sensors for space applications," *IEEE Trans. Microw. Theory Techn.*, vol. 65, no. 11, pp. 4450–4460, Nov. 2017.
[8] A. K. Jha, N. Delmonte, A. Lamecki, M. Mrozowski, and M. Bozzi, "Design of microwave-based angular displacement sensor," *IEEE Microw. Wireless Compon. Lett.*, vol. 29, no. 4, pp. 306–308, Apr. 2019.
[9] A. K. Jha, A. Lamecki, M. Mrozowski, and M. Bozzi, "A microwave sensor with operating band selection to detect rotation and proximity in the rapid prototyping industry," *IEEE Trans. Ind. Electron.*, vol. 68, no. 1, pp. 683–693, Jan. 2021.
[10] J. Tiemann, J. Pillmann, and C. Wietfeld, "Ultra-wideband antenna-induced error prediction using deep learning on channel response data," in *Proc. 85th Veh. Technol. Conf. (VTC Spring)*, 2017, pp. 1–5.
[11] A. R. J. Ruiz and F. S. Granja, "Comparing ubisense, bespoon, and decawave UWB location systems: Indoor performance analysis," *IEEE Trans. Instrum. Meas.*, vol. 66, no. 8, pp. 2106–2117, Aug. 2017.
[12] J. Tiemann and C. Wietfeld, "Scalability, real-time capabilities, and energy efficiency in ultra-wideband localization," *IEEE Trans. Ind. Informat.*, vol. 15, no. 12, pp. 6313–6321, Dec. 2019.
[13] P. Krapez, M. Vidmar, and M. Munih, "Distance measurements in UWB-radio localization systems corrected with a feedforward neural network model," *Sensors*, vol. 21, no. 7, p. 51, 2021.
[14] A. Narbudowicz, M. John, V. Sipal, X. Bao, and M. J. Ammann, "Design method for wideband circularly polarized slot antennas," *IEEE Trans. Antennas Propag.*, vol. 63, no. 10, pp. 4271–4279, Oct. 2015.
[15] L. Zhang *et al.*, "Single-feed ultra-wideband circularly polarized antenna with enhanced front-to-back ratio," *IEEE Trans. Antennas Propag.*, vol. 64, no. 1, pp. 355–360, Jan. 2016.
[16] Q. Liu, Z. N. Chen, Y. Liu, and C. Li, "Compact ultrawideband circularly polarized weakly coupled patch array antenna," *IEEE Trans. Antennas Propag.*, vol. 65, no. 4, pp. 2129–2134, Apr. 2017.
[17] A. Shlivinski, "Time-domain circularly polarized antennas," *IEEE Trans. Antennas Propag.*, vol. 57, no. 6, pp. 1606–1611, Jun. 2009.
[18] B. Y. Toh, R. Cahill, and V. F. Fusco, "Understanding and measuring circular polarization," *IEEE Trans. Educ.*, vol. 46, no. 3, pp. 313–318, Aug. 2015.
[19] P. J. Olver and C. Shakiban, *Application Linear Algebra* (Undergraduate Texts in Mathematics). Cham, Switzerland: Springer, 2018, doi: 10.1007/978-3-319-91041-3.
[20] V. Sipal, A. Narbudowicz, and M. J. Ammann, "Using near-field coupled circularly polarised antennas as frequency-independent variable phase shifters," *Electron. Lett.*, vol. 50, no. 11, pp. 788–790, May 2014.
[21] S. Genovesi, F. Costa, M. Borgese, F. A. Dicandia, and G. Manara, "Chipless radio frequency identification (RFID) sensor for angular rotation monitoring," *Technologies*, vol. 6, no. 3, p. 61, 2018.

Janusz Przewocki received the M.Sc. degrees in electrical engineering and applied mathematics from the Technical University of Gdansk, Gdansk, Poland, 2007 and 2009, and the Ph.D. degree in mathematics from the Polish Academy of Sciences, Warsaw, Poland, in 2015.

Since 2015, he has been an Assistant Professor with the University of Gdansk, Gdansk. He held a post-doctoral position at the Adam Mickiewicz University, Poznan, Poland, from 2017 to 2019. His fields of interests are applied topology, statistics, and geometrical methods in physics.

Max J. Ammann (Fellow, IEEE) received the Ph.D. degree in antennas and propagation from Trinity College Dublin, University of Dublin, Dublin, Ireland, in 1997.

He is currently a Professor of antennas and propagation with the School of Electrical and Electronic Engineering, Technological University Dublin, Dublin, where he is also the Director of the Antennas and High-Frequency Research Centre. He has served as an expert to industry on various antenna technologies in the communications, medical, aviation, and electronic security sectors in Ireland and abroad. He has more than 200 peer-reviewed papers published in journals and international conferences. His research interests broadly include electromagnetic theory, antenna miniaturization for terminal and ultra-wideband applications, antennas for medical devices, and antenna issues relating to privacy.

Dr. Ammann is a member of the IEEE International Committee for Electromagnetic Safety. His team received 13 best paper awards at international conferences on antennas and propagation and seven commercialization awards. He acted as an Associate Editor for the IEEE ANTENNAS AND WIRELESS PROPAGATION LETTERS (2012–2018). He became a Chartered Engineer in 1986.

Adam Narbudowicz (Member, IEEE) received the M.Sc. degree from the Gdansk University of Technology, Gdansk, Poland, in 2008, the Ph.D. degree from the Dublin Institute of Technology (now TU Dublin), Dublin, Ireland, in 2013, and the D.Sc. (habilitation) degree from the Wroclaw University of Science and Technology, Wroclaw, Poland, in 2020.

He is currently an SFI Starting Investigator at Trinity College Dublin, Dublin, and also an Associate Professor with the Wroclaw University of Science and Technology. He was a Post-Doctoral Fellow (twice) of Marie Skłodowska-Curie Action co-funded projects, including two-year research stay at RWTH Aachen University, Aachen, Germany. He has coauthored more than 70 scientific publications in journals and peer-reviewed conference proceedings. His research interests include antenna miniaturization for sensing and IoT applications, electrically small antennas, sustainable antenna technology, and antenna issues relating to privacy.

Dr. Narbudowicz received the Scholarship for the Outstanding Young Polish Scientists in 2019, the Inaugural 2018 Prof. Tom Brazil CONNECT Excellence in Research Award, the best poster by popular vote at the 2018 IEEE-EURASIP Summer School on Signal Processing, the 3rd Best Paper Award during ISAP 2017: International Symposium on Antennas and Propagation in 2017, and the DIT Inventor Competition Award for Best Postgraduate/Staff Invention in 2012. He was also a mentor to the finalist team of the 2020 IEEE APS Student Design Contest. He sits in the Management Committee of the COST action SyMat: "Future communications with higher-symmetric engineered artificial materials" and serves as the Vice-Chairperson for the IEEE Poland APS/MTT/AES Joint Chapter.